Eur Arch Otorhinolaryngol (2016) 273:1425–1431
DOI 10.1007/s00405-015-3705-7

OTOLOGY

Atypical radiographic features of skull base cholesterol granuloma

Christine T. Dinh[1] · Stefania Goncalves[1] · Rita Bhatia[2] · Kim Truong[1] · Fred Telischi[1] · Simon Angeli[1] · Jacques Morcos[2] · Adrien A. Eshraghi[1]

Received: 16 January 2015 / Accepted: 26 June 2015 / Published online: 12 July 2015

Abstract Cholesterol granulomas (CGs) are the most common benign lesions of the petrous apex (PA) and have distinct computed tomography (CT) and magnetic resonance imaging (MRI) characteristics. On CT, CGs of the PA (PACG) present as expansile lesions with erosion of bony trabeculae. MRI shows a hyperintense lesion on T1- and T2-weighted images and do not enhance with gadolinium. The objective is to describe the radiographic features of CGs of the skull base that do not arise from the PA. This study is a retrospective review. Three patients were operated on for suspected recurrent endolymphatic sac tumor, intracranial cholesteatoma, and recurrent sphenoid wing meningioma based on CT and MRI findings. Pathology results were consistent with CG in all three cases. All patients had bone erosion on CT. These skull base CGs did not demonstrate similar MRI features. These lesions were hyperintense, iso-to-hyperintense, and hypointense on T1-weighted MRI, respectively. These CGs were hyperintense in two cases and iso-to-hyperintense in one case on T2-weighted MRI. These lesions either demonstrated central or rim enhancement after gadolinium administration. Skull base CGs that do not arise from the PA demonstrate a broad spectrum of radiographic characteristics on MRI that are not typical of PACG.

Keywords Cholesterol granuloma · Petrous apex · Skull base · MRI · CT

✉ Adrien A. Eshraghi
aeshraghi@med.miami.edu

Christine T. Dinh
ctdinh@med.miami.edu

Stefania Goncalves
sxg376@med.miami.edu

Rita Bhatia
rbhatia@med.miami.edu

Kim Truong
truongkim8484@gmail.com

Fred Telischi
ftelischi@med.miami.edu

Simon Angeli
sangeli@med.miami.edu

Jacques Morcos
Jmorcos@med.miami.edu

[1] Department of Otolaryngology, University of Miami Miller School of Medicine, 1120 NW 14th Street, 5th Floor, Miami, FL 33136, USA

[2] Department of Neurosurgery, University of Miami Miller School of Medicine, 1611 NW 12th Avenue, Suite W279, Miami, FL 33136, USA

Introduction

Cholesterol granuloma (CG) is a cystic lesion formed by a foreign body giant cell reaction to cholesterol crystals and metabolized blood byproducts [1–4]. It is the most common benign lesion of the petrous apex (PA), the most medial portion of the temporal bone [1, 3]. There are two current theories about the pathogenesis of petrous apex cholesterol granulomas (PACG). The more historical theory is the obstructive-vacuum hypothesis which posits that the inflammatory reaction is secondary to mucosal swelling and obstruction of air cells, trapping of gas and subsequent negative pressure that causes extravasation of blood [2, 4]. The more recent theory is the exposed marrow hypothesis, which postulates that hyper-pneumatized apices allow exposure of bone marrow that may subsequently bleed and get sequestered in the air cells, which will undergo anaerobic metabolism leading to CG formation [2, 4].

PACGs demonstrate particular radiographic findings on computed tomography (CT) and magnetic resonance imaging (MRI) that are distinct from other lesions of the skull base. On CT, they are seen as a non-enhancing lesion centered at the PA that can expand and erode the adjacent bony trabeculae [1, 3, 5]. On both T1- and T2-weighted MRI, they have high signal intensity due to the presence of proteinaceous fluid, blood, and/or fat, and do not enhance with gadolinium [1, 3]. PACGs are often asymptomatic and frequently found incidentally on imaging. They may become symptomatic when the expansile mass erodes adjacent cortical bone and impinges on nearby structures, including the seventh and eighth cranial nerves (CN) as well as lower CNs [1–4]. The most common presenting clinical symptoms include hearing loss (65 %), vertigo (56 %), tinnitus (50 %), headaches (32 %), diplopia (6 %), and facial symptoms, such as paresthesia (21 %), twitching (24 %), and weakness (3 %) [1–5].

Asymptomatic CGs require no treatment but long-term follow-up with annual imaging is advisable. Treatment is indicated when lesions are growing or when patients become symptomatic [1, 3]. The standard treatment for symptomatic lesions is surgical drainage with or without silastic stenting to promote long-term aeration of the PA. Complete resection of the cyst is not usually possible due to the anatomical confines of the PA and risk of injury to adjacent critical structures [1, 3].

The differential diagnosis of PA and skull base lesions is broad and can include CG, cholesteatoma, mucocele, effusion, encephaloceles, diploic fatty marrow, petrous apicitis, and other benign or malignant tumors of the skull base, such as acoustic neuroma, meningioma, multiple myeloma, sarcoma, Langerhan's histiocytosis, and endolymphatic sac tumors (Table 1) [6]. Therefore, physicians rely on radiologic characteristics of the PA and skull base lesions to provide a diagnosis that will tailor initial treatment recommendations. We present three patients with skull base CG with atypical radiographic findings that underwent surgical intervention for suspected endolymphatic sac tumor, cholesteatoma, and meningioma, as suggested by radiographic features.

Case 1

This patient is a 40-year-old man who was referred to the Neurotology clinic for suspected recurrence of a right papillary endolymphatic sac tumor (ELST). He presented with right anacusis and tinnitus that resulted after a retrolabyrinthine approach for resection of an ELST at an outside hospital 5 years prior. His CN, head, and neck examinations were otherwise unremarkable. His most recent post-operative MRI demonstrated a vascular lesion located above the jugular bulb, adjacent to the endolymphatic duct, and abutting the posterior fossa dura that was not seen on prior imaging. The lesion was well-defined, lobulated, and measured 11.5 × 11.5 mm in the greatest

Table 1 Highlights the main differential diagnosis to consider when studying a pertrous apex lesion

CT	MRI	Additional features	Diagnosis
Non-expansile and non-destructive	T1, T2 hyperintense		Diploic fatty marrow
	T1 Iso to hyperintense or Iso to hypointense T2 hyperintense		Simple petrous apex effusion
	T1 hypointense, T2 hyperintense	In communication with Meckel's cave	Petrous apex cephalocele
Benign bony expansion	T1 hyperintense, T2 hyperintense, non-enhancing		Cholesterol granuloma (consider aneurysm)
	T1 Iso-to-hypointense, T2 hyperintense, non-enhancing	Increased signal-DWI	Cholesteatoma
		Decrease signal-DWI	Mucocele, rare cyst
	T1 Iso-to-hypointense, T2 hyperintense, enhancing		Rare benign tumor
Aggressive bony destruction	T1 Iso-to-hypointense, T2 Iso-to-hyperintense, enhancing	Clinical evidence of infections, middle ear disease, diabetes or immunosuppression	Petrous apicitis or central skull base osteomyelitis
		↑ Age	Metastasis, multiple myeloma
		↓ Age	Langerhan's cell histiocytosis, sarcoma
	T1 Iso-to-hypointense, T2 Iso-to-hyperintense, enhancing with areas of T1 hyperintensity, and location along posterior petrous apex.		Endolymphatic sac tumor

Adapted from: Connor et al. [6]

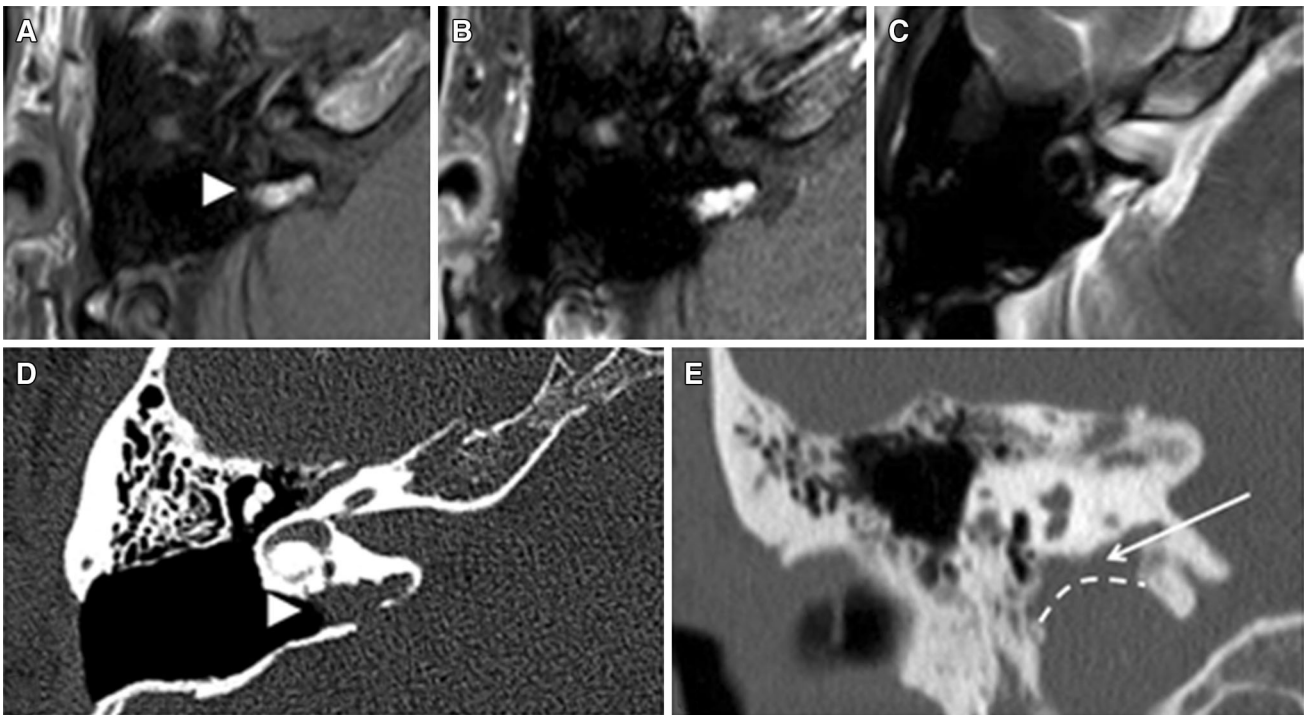

Fig. 1 Case 1: Radiographic findings of the right temporal bone. **a** Axial T1-weighted MRI at the level of the cochlea demonstrating a hyperintense lesion adjacent to the posterior fossa dura in the region of the endolymphatic sac (*arrowhead*). **b** This lesion enhances on axial T1-weighted MRI post contrast and with fat suppression. **c** This lesion is also hyperintense on axial T2-weighted MRI. **d** Axial CT scan at the level of the lateral semicircular canal demonstrating an erosive lesion adjacent to the endolymphatic duct (*arrowhead*). **e** Coronal CT scan of right temporal bone demonstrating the close proximity of the lesion (*arrow*) to a dehiscent jugular bulb (*dashed line*)

dimensions. This lesion was hyperintense on both T1- and T2-weighted images, enhanced with gadolinium, and did not restrict (low intensity signal) on diffusion-weighted images (DWI) of MRI (Fig. 1a–c). A CT of the temporal bone was performed and demonstrated bony erosion adjacent to the endolymphatic duct and soft tissue opacification in the area of the endolymphatic sac and posterior fossa dura (Fig. 1d). These findings were highly suspicious for recurrence of his ELST, and right revision translabyrinthine approach for resection of the ELST was performed. The pathology results were consistent with CG with dense fibroconnective tissue with no evidence of ELST or tumor.

Case 2

This patient is a 53-year-old man who presented to the Neurotology clinic with longstanding bilateral hearing loss, high-pitched tinnitus, otorrhea, and imbalance. He has several medical co-morbidities, including hypertension, hyperlipidemia, coronary artery disease with coronary stents, stroke with residual left arm weakness, iliofemoral bypass, and long-term use of anticoagulants. Physical examination demonstrated significant bilateral tympanic membrane retraction onto the ossicular chain and promontory that were dry. No nystagmus could be elicited on physical examination, but he swayed with Fukuda stepping and Romberg tests. His audiogram demonstrated bilateral mixed hearing loss with excellent word recognition. His temporal bone CT showed bilateral opacification of the middle ear and mastoid as well as a large dehiscence of the right tegmen tympanicum (Fig. 2a, b). There was blunting of the scutum and ossicular erosion bilaterally. Brain MRI demonstrated a well-circumscribed lesion in the right middle cranial fossa with soft tissue density extending down into the epitympanum. This lesion was iso-to-hyperintense on T1-weighted images, hyperintense on T2-weighted images, did not restrict with DWI, and demonstrated subtle rim enhancement with administration of gadolinium (Fig. 2c–e). A similar but significantly smaller lesion involving only the left epitympanum was also seen on MRI. The patient underwent a right mastoidectomy and middle cranial fossa craniotomy to remove a suspected right ear and intracranial cholesteatoma. Intraoperatively, intentional incision into the mass demonstrated a thick

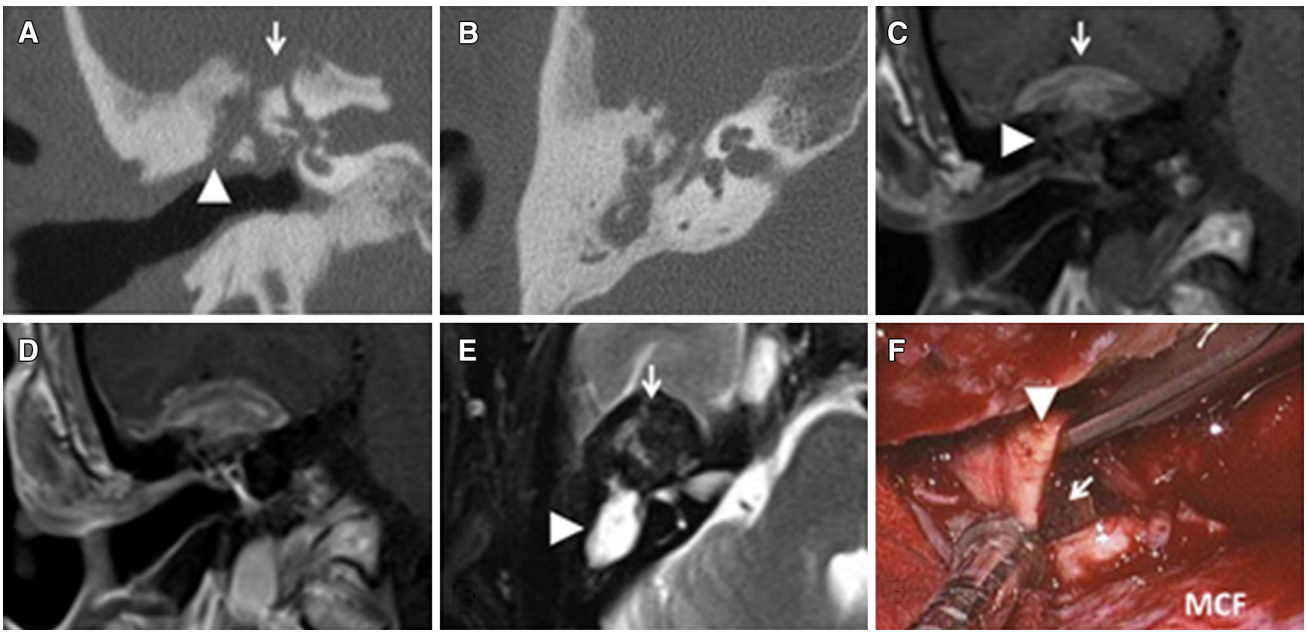

Fig. 2 Case 2: Radiographic and surgical findings of the right temporal bone. **a**. Coronal CT scan at the level of the external auditory canal demonstrating erosion of the scutum (*arrowhead*) and tegmen tympanicum (*arrow*). **b** Axial CT scan at the level of the cochlea demonstrates opacification of the middle ear and mastoid. **c** Coronal T1-weighted MRI at the level of the external auditory canal demonstrating an irregular iso-to-hyperintense lesion involving the epitympanum (*arrowhead*) and middle cranial fossa (*arrow*). **d** Coronal T1-weighted MRI post contrast showing some subtle rim enhancement. **e** Axial T2-weighted MRI at the level of the cochlea showing an irregular heterogeneous lesion with areas of hyperintensity (*arrowhead*) and hypointensity (*arrow*). **f**. Image of CG capsule (*arrowhead*) with intracapsular blood byproducts (*arrow*) adjacent to dura of the right middle cranial fossa (MCF)

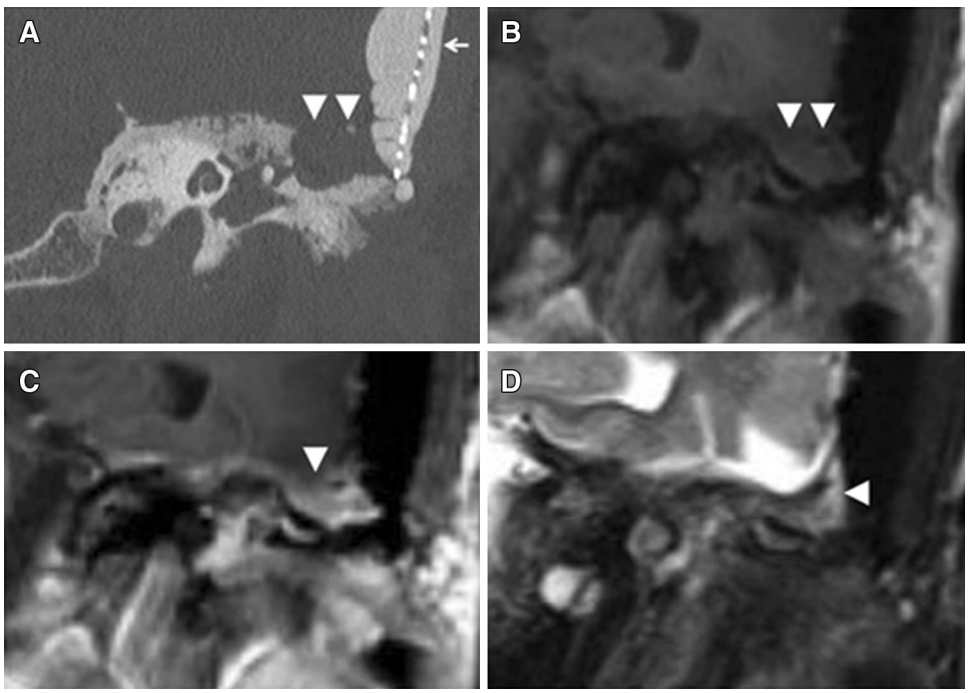

Fig. 3 Case 3: Radiographic findings of left temporal bone. **a** Coronal CT scan at the level of the cochlea demonstrating dehiscence at the tegmen mastoideum (*arrowheads*), previous cranioplasty (*arrow*), and middle ear opacification. **b** Coronal T1-weighted MRI at the level of the cochlea demonstrating a hypointense lesion involving the mastoid bone (*arrowheads*). **c** This dural-based lesion enhances with gadolinium on coronal T1-weighted MRI. **d** This lesion is iso-to-hyperintense on coronal T2-weighted MRI

Table 2 Highlights the main CT and MRI findings of typical PACG, ELSTs, cholesteatoma, meningioma, and our three case presentations for comparison

	CT	T1	T1 + Gad	T2	DWI
PACG	Expansile soft tissue lesion at PA	Hyper	Does not enhance	Hyper	Normal
Case 1 CG	Retrolabyrinthine bone erosion	Hyper	Enhances	Hyper	Normal
Case 2 CG	Scutum and ossicular erosion Opacification of epitympanum	Iso to hyper	Subtle rim enhancement	Hyper	Normal
Case 3 CG	Tegmen dehiscence Mastoid opacification	Hypo	Enhances	Iso to hyper	Normal
ELST	Retrolabyrinthine bone erosion Intratumoral calcifications	Hyper	Enhances	Hyper	Normal
Cholesteatoma	Scutum and ossicular erosion Opacification of epitympanum	Hypo	Does not enhance	Hyper	Restricts
Meningioma	Calcifications Hyperostosis	Hypo to Iso	Enhances	Iso to hyper	Normal

The three cases presented with atypical radiographic findings for CG

capsule with old appearing blood contents within the lumen (Fig. 2f). The surgical pathology contained dense connective tissue with cholesterol clefts, hemosiderin, calcification, and foreign body multinucleated giant cells, consistent with CG.

Case 3

This patient is a 51-year-old female with a history of left lateral sphenoid wing meningioma involving the left middle cranial fossa that was resected 1 year ago via a transtemporal approach requiring zygomatic osteotomies. Residual tumor was purposefully left in the left cavernous sinus and Meckel's cave to minimize morbidity, and a large cranioplasty with titanium mesh was performed to repair the surgical defect. She presented to the Neurotology clinic for persistent left otalgia despite several courses of antibiotics. On physical examination, she had postsurgical scars that were well healed, a left aural polyp that was obscuring visualization of the tympanic membrane, and decreased sensation of her left face (CN V1–V3 distribution). Her audiogram demonstrated a conductive hearing loss in the left ear with excellent word recognition. Her temporal bone CT scan showed extensive hyperostosis of the temporal bone, prior left temporal cranioplasty, bony defect of the left tegmen mastoideum (Fig. 3a), opacification of the left middle ear and mastoid bone, and soft tissue density in the external auditory canal with erosion of the bone posteriorly. Brain MRI demonstrated a lesion of the left mastoid bone, adjacent to the tegmen dehiscence. This dural-based lesion was hypointense on T1-weighted MRI, iso-to-hyperintense on T2-weighted MRI, and enhanced with gadolinium, suggesting possible recurrence of her previously resected meningioma (Fig. 3b–d). She was taken to the operating room for a modified radical mastoidectomy, tympanoplasty, and revision middle cranial fossa approach for resection of the aural polyp and suspected recurrence of meningioma. The aural polyp was found to be secondary to an external auditory canal cholesteatoma and the dural base lesion was confirmed to be CG on histopathology.

Discussion

CG is a cystic lesion that most commonly occurs in the PA from metabolism of blood byproducts and foreign body giant cell reaction to cholesterol crystals [1–4]. CGs that occur in the PA demonstrate very distinct features on CT and MRI. On CT scan imaging, they present as smooth, well-defined, expansile lesions that can erode the bony septations of the PA. Due to accumulation of proteinaceous fluid and blood byproducts, PACG are hyperintense on T1- and T2-weighted MRI [1, 3]. Although CGs do not typically enhance with gadolinium, due to a local inflammatory response, a peripheral enhancement can sometimes be seen with contrast administration [7]. We report three cases of skull base CG that do not demonstrate the usual radiographic characteristics of PACGs (Table 2).

ELSTs are rare, slow growing, low-grade, and locally aggressive tumors of the temporal bone. Because they are slowly progressive tumors, there is usually an indolent clinical course until extensive bony erosion has occurred. A majority of ELSTs occur sporadically; however, this entity is associated with 11 % of cases with Von-Hippel-Lindau syndrome [8, 9]. On CT scan, ELSTs usually demonstrate soft tissue density with internal calcifications with various degrees of bony destruction in the retrolabyrinthine area

where the endolymphatic sac is situated. On MRI, ELSTs can demonstrate heterogeneity and hyperintensities on T1- and T2-weighted MRI due to intratumoral bleeding [9], can enhance with gadolinium, and can show flow voids. Case 1 had several clinical and radiographic features of recurrent ELST (Table 1); however, the final pathology was consistent with CG and dense fibroconnective tissue without evidence of tumor. These atypical radiographic findings for CG may be associated with the inflammatory features of the dense fibroconnective tissue, while development of the CG may be result of occult bleeding from the dehiscent jugular bulb after the initial surgery 5 years ago. Enhancement of the lesion on T1 MRI with gadolinium suggested tumor recurrence; however, enhancement may occur with inflammatory response and fibroconnective tissue formation.

Cholesteatoma occurs when there is abnormal growth of squamous epithelium in the middle ear and mastoid. They can present as congenital epithelial cysts, as a result of iatrogenic insertion of squamous cells into the middle ear following procedures involving the tympanic membrane, or from chronic Eustachian tube dysfunction and tympanic membrane retractions that result in squamous lined pockets. The lining of the cyst or sac comprises squamous epithelium that can desquamate, produce keratin debris, become infected, and promote an inflammatory reaction that lead to local bone erosion. On high resolution CT, cholesteatoma is usually seen as a soft tissue density within the epitympanum and at the pars flaccida that is eroding the bony scutum and/or ossicles. On MRI, cholesteatomas are often hypointense on T1-weighted MRI, hyperintense on T2-weighted images, and restrict on DWI [10]. Central enhancement with gadolinium is not common but a peripheral enhancing rim is sometimes seen in the presence of inflammation or infection. Case 2 had several clinical and radiographic features suggestive of cholesteatoma (Table 2); however, surgical and histopathological examinations of the lesion were consistent with CG of the skull base. In particular, the patient had bilateral epitympanic lesions with retracted tympanic membranes and scutum erosion suggestive of cholesteatoma. The etiology of the CG is unknown; however, the patient has an extensive history of using anticoagulants which may contribute to the formation of this CG lesion. A low-grade infection or super-imposed inflammation from his chronic Eustachian tube dysfunction and resultant chronic otitis media may - have altered the classic radiographic appearance of this CG cyst. Additionally, bilateral presentation of this CG is also atypical and only seven cases have been reported in the literature [11–17]. There is only one reported case with bilateral intracranial presentation [15].

Meningiomas are slow growing tumors that arise from the meningothelial cells of the arachnoid and account for approximately 16–20 % of all intracranial tumors [18]. Most meningiomas are asymptomatic but can become symptomatic as they grow and compress adjacent structures. These tumors are best visualized with MRI and appear as well-circumscribed lesions that are hypo- to isointense on T1-weighted MRI, iso-to-hyperintense on T2-weighted MRI, and enhance with gadolinium. Intratumoral calcifications can also be present on CT scan [18]. In case 3, the patient had a history of prior meningioma resection of the middle cranial fossa and presented with an enhancing lesion in the mastoid adjacent the surgical bed. The lesion was hypointense on T1-weighted MRI and iso-to-hyperintense on T2-weighted MRI. Given the clinical scenario and enhancing lesion near the surgical bed, recurrent meningioma was high on the differential diagnosis. Surgical and histopathologic evaluations of this enhancing lesion at the skull base were consistent with CG, suggesting that skull base CG can present with hypointensity on T1-weighted images, can demonstrate central enhancement, and can masquerade as a meningioma (Table 2). Occult bleeding into the mastoid from the prior middle cranial fossa operation may have contributed to the formation of this CG, while a super-imposed infection with inflammation from the external auditory canal cholesteatoma may contributed to the atypical features of CG.

These three case reports demonstrate that skull base CGs that do not occur in the PA can have radiographic findings that are not usual for a PACG. CGs that do not occur in the PA can be hypointense, isointense, or hyperintense on T1-weighted MRI; they can also be iso-to-hyperintense on T2-weighted images and demonstrate rim or central enhancement with gadolinium. Furthermore, all three of these patients had bone erosion on CT, which is not typical of PACG. The spectrum in radiographic characteristics of these three skull base CGs is broad but all patients had different risk factors that contribute to formation of CG.

The patient in case 1 presented with CG 5 years after initial surgery; however, this lesion is in very close proximity to a dehiscent jugular bulb, which may represent a source of bleeding that promotes formation of CG. The dense fibroconnective tissue formation may have affected classical radiographic features of CG in patient 1. Patient 2 had an extensive history of anticoagulant intake secondary to extensive cardiovascular disease and possibly low-grade inflammation from his chronic Eustachian tube dysfunction and chronic otitis media that affected the radiologic findings. The patient in case 3 had intracranial surgery within one year of presentation suggesting that retained blood products in the mastoid may have initiated the event; a super-imposed infection and inflammatory response from the external auditory canal cholesteatoma may have obscured usual radiographic characteristics of CG.

The classical radiographic features of CG may be more obvious when the cystic component predominates over the granulomatous component. The skull base CGs presented in our case series were likely associated with an underlying inflammation from previous surgery, chronic otitis media, or active infection, which support the theory that inflammation and granulation may affect the usual radiographic characteristics of a CG.

This study is limited by a small sample size given that CGs are rare in general; larger numbers of patients and case-controlled studies are necessary to further elucidate this subset of skull base CGs and their radiographic differences from PACGs.

Conclusion

Skull base CGs that do not arise from the PA demonstrate a very broad spectrum of radiographic characteristics, particularly with MRI. We present three cases of CG arising at the base of skull that do not have the typical radiographic features of PACG, suggesting that skull base CGs outside the PA may represent a different pathophysiologic entity than PACG that is associated with inflammation and infection. Further study of the CT and MRI features in skull base CGs that do not originate in the PA may shed insight on the pathophysiology behind these lesions.

References

1. Brackmann D, Toh E (2002) Surgical management of petrous apex cholesterol granulomas. Otol Neurotol 23:529–533
2. Jackler RK, Cho M (2003) A new theory to explain the genesis of petrous apex cholesterol granuloma. Otol Neurotol 24:96–106
3. Narayan A, Jain R, Chwang W, Seidman M, Rock J (2012) Hemorrhagic petrous apex cholesterol granuloma. Arch Otolaryngol Head Neck Surg 138(12):1180–1183
4. Yamil S, Wood J, Telischi F, Casiano R, Angeli S (2013) Development of cholesterol granuloma in a temporal bone petrous apex previously containing marrow exposed to air cells. Otol Neurotol 34:958–960
5. Hoa M, House JW, Linthicum FH, Go JL (2013) Petrous apex cholesterol granuloma: pictorial review of radiological considerations in diagnosis and surgical histopathology. J Laryngol Otol 127(4):339–348
6. Connor SEJ, Leung R, Natas S (2008) Imaging of the petrous apex: a pictorial review. Br J Radiol 81:427–435
7. Royer MC, Pensak ML (2007) Cholesterol granulomas. Curr Opin Otolaryngol Head Neck Surg 15:319–322
8. Alkonyi B, Gunthner-Lengfeld T, Rak K, Nowak J, Solymosi L and Hagen Rudolf (2014) An endolymphatic sac tumor with imaging features of aneurysmal bone cysts: differential diagnostic considerations. Childs Nerv Syst [Epub ahead of print]
9. Megerian CA, Semaan MT (2007) Evaluation and management of endolymphatic sac and duct tumors. Otolaryngol Clin N Am 40:463–478
10. Corrales CE, Blevins NH (2013) Imaging for evaluation of cholesteatoma: current concepts and future directions. Curr Opin Otolaryngol Head Neck Surg 21(5):461–467
11. Masaany M, Siti HS, Murliza I, Mazita A (2008) Bilateral middle ear cholesterol granuloma in familial hypercholesterolemia. Otolaryngol Head Neck Surg 138(6):803–804
12. Kuo SW, Cheng PW, Yang LH (2006) Bilateral giant cholesterol granuloma of the temporal bones. Otol Neurotol 27(8):1197–1198
13. Eby TL, Guthrie BL (1998) Bilateral cholesterol granulomas of the temporal bone ORL. J Otorhinolaryngol Relat Spec 60(6):318–321
14. Linstrom CJ, McLure TC 3rd, Gamache FW Jr, Saint-Louis LA (1989) Bilateral cholesterol granulomas of the petrous apices: case report and review. Am J Otol 10(5):393–401
15. Henick DH, Feghali JG (1994) Bilateral cholesterol granuloma: an unusual presentation as an intradural mass. J Otolaryngol 23(1):15–18
16. Verret DJ, Samy RN (2005) Bilateral cholesterol granulomas. Otol Neurotol 26(5):1041–1044
17. Gamache FW Jr, McLure T, Deck M, Linstrim C (1988) Bilateral cholesterol granuloma of the skull base: case report and review of the literature. Neurosurgery 22(6 Pt 1):1098–1101
18. Watts J, Box G, Galvin A, Brotchie P, Trost N, Sutherland T (2014) Magnetic resonance imaging of meningiomas: a pictorial review. Insights Imaging 5(1):113–122